*Magazine of Concrete Research*, 2008, **60**, No. 2, March, 109–118
**doi:** 10.1680/macr.2008.60.2.109

# Measurement of early-age temperature rises in concrete made with blended cements

R. K. Dhir, L. Zheng and K. A. Paine

*University of Dundee*

*The advisability of controlling the temperature rise and fall in concrete at early age is well recognised as one of the factors preserving long-term performance and durability of structures. Of particular importance in design of water-retaining and massive concrete structures is $T_1$, the difference between peak temperature of the section and mean ambient temperature. In previous studies, a cement hydration model was developed in order to predict $T_1$ for concrete made with low heat (LH) and very low heat (VLH) special cements. To test this model, a study was carried out to measure the early-age temperature rises for concrete elements containing blended cements, meeting the requirements for the LH and VLH classes. The effects of cement heat class, cement content, formwork type and section thickness on the temperature rise were evaluated for both cement types. Verification of the established models was evaluated by comparing measured temperature rises with those predicted. It was found that the model proposed in previous studies gave satisfactory prediction of $T_1$ values.*

## Introduction

The advisability of controlling the temperature rise and fall in concrete at early age is well recognised as one of the factors preserving long-term performance and durability of structures. When the difference between the peak temperature inside the concrete core and the mean ambient temperature is large, temperature gradients across the concrete section can initiate cracking. If these cracks are not minimised and crack widths controlled, serviceability may be seriously affected, particularly with respect to water-retaining structures.

One widely used method to reduce thermal cracking is to use cements with low heat of hydration characteristics. Indeed, in the European standards BS EN 197-1[1] and BS EN 197-4,[2] a single class of low heat (LH) cement has been defined in order to assist engineers in the selection of appropriate materials. In addition, BS EN 14216[3] defines very low heat (VLH) special cements as those which, through composition, fineness and reactivity of constituents, have a slower early hydration process than LH cements, and which are particularly suitable for dams and other massive structures that have a low surface/volume ratio.

At present, however, engineers are unable to take full advantage of these cement classes because there is a lack of test data for cements meeting the specific limits, and the classes cannot be used in conjunction with current design guidance.[4–6] Recognising this, an extensive revision to CIRIA R91[6] has recently been carried out by Bamforth, as CIRIA C660,[7] to include guidance for use of blended cements and combinations meeting the LH and VLH classes. This revision has derived design data by using a model and computer program devised by the University of Dundee.[8,9] Because the use of blended cements and combinations to achieve low heat cements is worldwide practice, for example ASTM C 595,[10] AS 3972[11] and GB 200,[12] the model and subsequent data are also applicable to non-European practice.

The current paper describes a study carried out to verify the accuracy of the design data determined by the model and program, by comparing predictions of $T_1$, the temperature fall from peak to mean ambient, with values measured on a number of concrete elements containing blended cements falling within the LH and VLH classes. Tests were carried out to assess the effects of cement heat class, cement content, formwork type and section thickness for a range of blended cements.

Concrete Technology Unit, Division of Civil Engineering, University of Dundee, UK, DD1 4HN

(MACR-D-00034) Paper received 9 January 2007; revised 30 August 2007; accepted 18 September 2007



www.concrete-research.com 1751-763X (Online) 0024-9831 (Print) 

## Temperature profile calculation model

The heat of hydration model used in the present paper was developed in response to the incorporation of heat classes in the European standards for cement, and was specifically designed to allow the effect of blended cement composition to be taken into account. This was required because a review had indicated that current models in the literature[13–18] were either: (*a*) over-complicated, requiring a large number of parameters that are not available in general engineering practice; for example cement mineral compositions, that is $C_3S$, $C_2S$, $C_3A$ and $C_4AF$ content, and their particle sizes; or (*b*) did not allow the non-PC content in cement combinations to be varied. A full description of the model is given elsewhere[8] and it is based on the Arrhenius function and refined De Schutter functions.[19]

The program for calculating the early-age temperature profile of concrete is based on this model and general heat flow theory,[20,21] and the variable parameters within the program are cement content, formwork type, section size, ambient temperature and placing temperature. Other parameters including the specific heat capacity and thermal conductivity of concrete, and the convection heat transfer coefficient may be adjusted if necessary.

It is assumed from general heat flow theory that the temperature distribution in a concrete cross-section, at any point in time, is the dynamic heat balance between the heat generated inside the concrete and the heat lost to, or gained from, the ambient. The temperature distribution within a concrete body or the momentary heat flow within the boundaries of the body is governed by the well-known Fourier law, which is given as the following differential equation

$$\frac{\partial T}{\partial t} = \frac{K}{\rho c}\left(\frac{\partial^2 T}{\partial x^2} + \frac{\partial^2 T}{\partial y^2} + \frac{\partial^2 T}{\partial z^2}\right) + q(x, y, z, t) \quad (1)$$

where $T$ is temperature, °C; $t$ is time; $K$ is the thermal conductivity of concrete, W/mK; $q$ is the rate of heat generated inside the concrete body, W/m$^3$; $\rho$ is the density of concrete, kg/m$^3$; $c$ is the specific heat of concrete, J/gK; and $x$, $y$, $z$ are Cartesian coordinates in the $x$, $y$ and $z$ directions.

For one-dimensional calculations, the solution to the Fourier differential equation was achieved using a finite-difference method.[22] Fig. 1 shows the simplified concrete model for temperature calculation. One element was considered for the formwork and the concrete wall was divided into $n$ elements from the concrete surface to the centre. During the calculation, temperature values, $T_n$, at time step $m + 1$ are calculated based on the results obtained at the previous time step $m$ and the calculation formulae are as follows

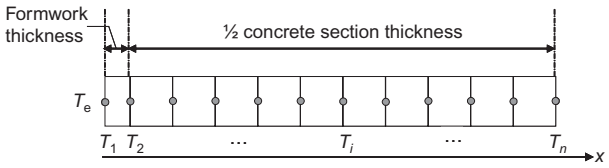


*Fig. 1. Division of the concrete wall into elements*

$$T_1^{m+1} = T_1^m - \frac{2\Delta t}{\Delta x_1 \rho_1 c_1}\left[\frac{K_1(T_1^m - T_2^m)}{\Delta x_1} + h(T_1^m - T_e^m)\right]$$

$$T_2^{m+1} = T_2^m - \frac{2\Delta t}{(\Delta x_1 \rho_1 c_1 + \Delta x_2 \rho_2 c_2)}\left[\frac{K_1(T_2^m - T_1^m)}{\Delta x_1} + \frac{K_2(T_2^m - T_3^m)}{\Delta x_2} - \frac{\Delta x_2}{2}\Delta QC\right]$$

$$T_i^{m+1} = T_i^m - \frac{\Delta t}{\Delta x_2 \rho_2 c_2}\left[\frac{K_2(T_i^m - T_{i-1}^m)}{\Delta x_2} + \frac{K_2(T_i^m - T_{i+1}^m)}{\Delta x_2} - \Delta x_2 \Delta QC\right]$$

(for $i = 3$ to $n - 1$)

$$T_n^{m+1} = T_n^m - \frac{2\Delta t}{\Delta x_2 \rho_2 c_2}\left[\frac{K_2(T_n^m - T_{n-1}^m)}{\Delta x_2} - \frac{\Delta x_2}{2}\Delta QC\right] \quad (2)$$

where $\Delta t$ is the interval; $h$ is the convection heat transfer coefficient; $K_1$, $\rho_1$, $c_1$ are thermal conductivity, density and specific heat of formwork, respectively; $K_2$, $\rho_2$, $c_2$ are thermal conductivity, density and specific heat of concrete, respectively; $\Delta x_1$, $\Delta x_2$ are element thickness of formwork and concrete, respectively; $\Delta Q$ is heat generated in the concrete element during the time interval; and $C$ is the cement content of the concrete.

Calculations used to determine $\Delta Q$ in equation (2) were attained from the heat of hydration model and based on isothermal calorimetry tests carried out on Portland cement (PC), PC/fly ash cements and PC/ground granulated blastfurnace slag (ggbs) cements.[8] The total heat evolution of cements was considered to be the sum of three components, *viz.* (a) the heat from an initial PC reaction, (b) a latent hydraulic ggbs reaction and (c) co-reactivity effects between the PC and ggbs, or PC and fly ash.

For two-dimensional calculations, the solution was achieved using a finite-element method (FEM): the heat of hydration model and the time step treatment of the calculation programme were the same as for the one-dimensional calculation; however, an object finite-element library (OFELI), developed by Touzani,[23] was used. It has been reported in the literature that a commercial FEM package can be used in two-dimensional calculations;[24] however this

FEM package only allows input curves of rate of heat generated plotted against time. This makes it unsuitable for modelling cement hydration, where the rate of heat generation depends not only on time but also on the history of hydration—that is, the total heat that has been generated. Therefore, it is necessary to develop some special sub-routines to meet the requirements of the hydration models.

The thermal properties used in the program are given in Table 1. Values of 1·02 J/gK for the specific heat capacity and 3·5 W/mK for the thermal conductivity of concrete represent typical values for natural gravel concretes at the point at which the maximum temperature in the concrete is reached.[25]

*Table 1. Physical constants used in the program*

| Constant | Concrete | Timber | Steel |
|---|---|---|---|
| Thermal conductivity: W/mK | 3·5 | 0·18 | 50 |
| Specific heat: J/gK | 1·02 | 1·63 | 0·42 |
| Density: kg/m$^3$ | 2400 | 650 | 7800 |

## Experimental programme of work

Experimental measurement of the early-age temperatures in 32 laboratory-cast concrete elements was carried out. Parameters investigated were cement type (PC/ggbs or PC/fly ash), ggbs or fly ash content, total cement content (250 kg/m$^3$ or 400 kg/m$^3$), formwork type (plywood or steel) and section thickness (250 mm, 500 mm or 750 mm). In total, eight different concrete mixes were prepared and four elements cast from each mix. Table 2 gives the test arrangement for each element.

Blended cements were produced by combining PC with various proportions of ggbs or fly ash to produce cements characteristic of factory-made cements or concrete combinations of the same composition currently available in the UK. The materials used were: (*a*) PC, strength class 42.5 N conforming to BS EN 197-1,[1] (*b*) ggbs conforming to BS 6699[26] and (*c*) fly ash conforming to BS 3892–1.[27] The physical and chemical properties of PC, ggbs and fly ash are shown in Table 3.

PC/ggbs and PC/fly ash cements were prepared to meet the LH and VLH classes as defined in BS EN 197-1[1] and BS EN 14216.[3] Previous work had

*Table 2. Test arrangement for concrete column tests*

| Test code | Heat class | ggbs or fly ash content: % by mass | Cement content: kg/m$^3$ | Formwork type | Minimum section thickness: mm |
|---|---|---|---|---|---|
| A1 | VLH | 70% ggbs | 400 | Plywood | 750 |
| A2 | VLH | 70% ggbs | 400 | Steel | 500 |
| A3 | VLH | 70% ggbs | 400 | Plywood | 500 |
| A4 | VLH | 70% ggbs | 400 | Plywood | 250 |
| B1 | VLH | 70% ggbs | 250 | Plywood | 750 |
| B2 | VLH | 70% ggbs | 250 | Steel | 500 |
| B3 | VLH | 70% ggbs | 250 | Plywood | 500 |
| B4 | VLH | 70% ggbs | 250 | Plywood | 250 |
| C1 | LH | 45% ggbs | 400 | Plywood | 500 |
| C2 | LH | 45% ggbs | 400 | Steel | 750 |
| C3 | LH | 45% ggbs | 400 | Steel | 500 |
| C4 | LH | 45% ggbs | 400 | Steel | 250 |
| D1 | LH | 45% ggbs | 250 | Plywood | 500 |
| D2 | LH | 45% ggbs | 250 | Steel | 750 |
| D3 | LH | 45% ggbs | 250 | Steel | 500 |
| D4 | LH | 45% ggbs | 250 | Steel | 250 |
| E1 | VLH | 50% fly ash | 400 | Plywood | 750 |
| E2 | VLH | 50% fly ash | 400 | Steel | 500 |
| E3 | VLH | 50% fly ash | 400 | Plywood | 500 |
| E4 | VLH | 50% fly ash | 400 | Plywood | 250 |
| F1 | VLH | 50% fly ash | 250 | Plywood | 750 |
| F2 | VLH | 50% fly ash | 250 | Steel | 500 |
| F3 | VLH | 50% fly ash | 250 | Plywood | 500 |
| F4 | VLH | 50% fly ash | 250 | Plywood | 250 |
| G1 | LH | 30% fly ash | 400 | Plywood | 500 |
| G2 | LH | 30% fly ash | 400 | Steel | 750 |
| G3 | LH | 30% fly ash | 400 | Steel | 500 |
| G4 | LH | 30% fly ash | 400 | Steel | 250 |
| H1 | LH | 30% fly ash | 250 | Plywood | 500 |
| H2 | LH | 30% fly ash | 250 | Steel | 750 |
| H3 | LH | 30% fly ash | 250 | Steel | 500 |
| H4 | LH | 30% fly ash | 250 | Steel | 250 |

*Table 3. Properties of PC, ggbs and fly ash used in study*

| Property | PC | ggbs | Fly ash |
|---|---|---|---|
| Relative density | 3·14 | 2·88 | 2·14 |
| Fineness: $m^2/kg$ | 405 | 466 | 7·2 * |
| Particle size distribution: % passing by volume | | | |
| 125 μm | 100·0 | 100·0 | 100·0 |
| 100 μm | 100·0 | 99·9 | 99·8 |
| 75 μm | 99·8 | 99·6 | 97·7 |
| 45 μm | 96·6 | 96·6 | 88·7 |
| 25 μm | 81·8 | 84·9 | 70·9 |
| 10 μm | 41·2 | 53·7 | 41·6 |
| 5 μm | 19·7 | 34·5 | 24·6 |
| 2 μm | 7·7 | 17·1 | 10·9 |
| 1 μm | 4·3 | 8·1 | 5·5 |
| 0·7 μm | 2·4 | 4·1 | 3·0 |
| 0·5 μm | 0·8 | 1·3 | 1·0 |
| 0·2 μm | 0·1 | 0·1 | 0·1 |
| Bulk oxide composition | | | |
| $SiO_2$ | 21·5 | 36·3 | 44·2 |
| $Al_2O_3$ | 5·4 | 12·6 | 29·0 |
| $Fe_2O_3$ | 2·6 | 0·5 | 5·9 |
| CaO | 64·2 | 42·1 | 2·2 |
| MgO | 2·6 | 6·9 | 0·9 |
| $P_2O_5$ | 0·1 | 0·0 | 0·6 |
| $TiO_2$ | 0·3 | 0·6 | 1·5 |
| $SO_3$ | 2·8 | – | 0·6 |
| $K_2O$ | 0·7 | 0·3 | 1·2 |
| $Na_2O$ | 0·3 | 0·2 | 0·2 |
| MnO | 0·0 | 0·3 | 0·0 |

* % by mass retained on 45 μm sieve—wet sieving

calculated the ggbs and fly ash contents that meet these classes.[10] Subsequently, the LH cements contained 45% ggbs or 30% fly ash by mass of cement, and the VLH cements contained 70% ggbs and 50% fly ash by mass of cement.

Concrete mix proportions are given in Table 4. The coarse aggregates used were natural gravels of 20 mm maximum size, in two single-size fractions, 20–10 mm and 10–5 mm conforming to BS EN 12620.[28] Fine aggregates used were natural sands conforming to BS EN 12620. The cube strength and flexural strength for each mix are given in Table 5.

Figure 2 shows a typical section for the moulds used (250 mm). Note that a section thickness of 250 mm refers to the minimum section thickness, since the other dimensions were 500 mm and 1000 mm. For moulds with other section thicknesses, the general design was similar. The inner dimensions for the moulds of section thickness 500 mm and 750 mm were $500 \times 750 \times 1000$ mm and $750 \times 1000 \times 1000$ mm, respectively. The top and bottom faces were covered with an insulating styrofoam sheet to avoid transfer of heat vertically.

Thermocouples, made of nickel chromium/nickel aluminium alloys, were used to measure the temperature changes inside the concrete section. The measured temperatures at different points were recorded by a data-logger. For elements with section thickness of 500 mm or 750 mm, five temperature measuring points in the concrete section were arranged and numbered as shown in Fig. 3. Thermocouple 1 (Therm1) was used to measure the temperature at the centre of the specimen. Therm3 and Therm5 were used to measure the temperature of the inside surface of the formwork. Therm2 and Therm4 were at the halfway point between the surface and the centre of the specimen. For elements with section thickness of 250 mm, only three temperature measurements were taken, with Therm2 and Term4 omitted owing to the small section. During testing, ambient temperature was measured from three points around the specimen and data-logger. For some selected elements, temperatures on the outside surface of the formwork were also measured.

## Results and discussions

Typical temperature profiles of the concrete elements are shown in Figs 4 and 5. Tables 6 and 7 give a summary of data for each of the 32 elements tested

*Table 4. Concrete mix proportions for column tests*

| Concrete mix code | Concrete mix proportions: $kg/m^3$ | | | | | | | |
|---|---|---|---|---|---|---|---|---|
| | Water | PC | ggbs or fly ash | Total Cement | w/c | Aggregates | | |
| | | | | | | Fine | 10 mm | 20 mm |
| ggbs concrete | | | | | | | | |
| A (VL, 70% ggbs) | 185 | 120 | 280 | 400 | 0·46 | 615 | 400 | 800 |
| B (VL, 70% ggbs) | 180 | 75 | 175 | 250 | 0·72 | 750 | 400 | 800 |
| C (L, 45% ggbs) | 185 | 220 | 180 | 400 | 0·46 | 615 | 400 | 800 |
| D (L, 45% ggbs) | 180 | 135 | 115 | 250 | 0·72 | 750 | 400 | 800 |
| Fly ash concrete | | | | | | | | |
| E (VL, 50% fly ash) | 170 | 200 | 200 | 400 | 0·43 | 630 | 400 | 800 |
| F (VL, 50% fly ash) | 165 | 125 | 125 | 250 | 0·66 | 780 | 400 | 800 |
| G (L, 30% fly ash) | 170 | 280 | 120 | 400 | 0·43 | 630 | 400 | 800 |
| H (L, 30% fly ash) | 165 | 175 | 75 | 250 | 0·66 | 780 | 400 | 800 |

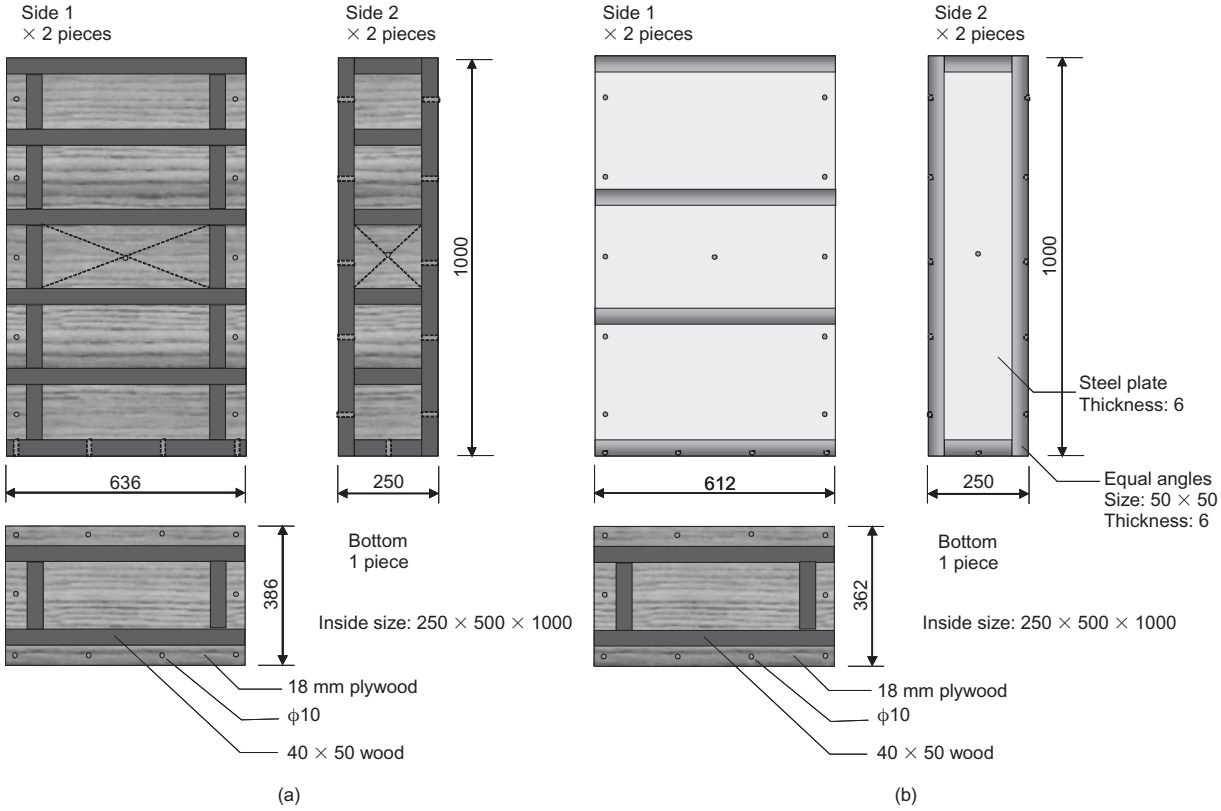


*Fig. 2. Design charts for formworks with section thickness of 250 mm: (a) plywood formwork; (b) steel formwork (all dimensions in mm)*

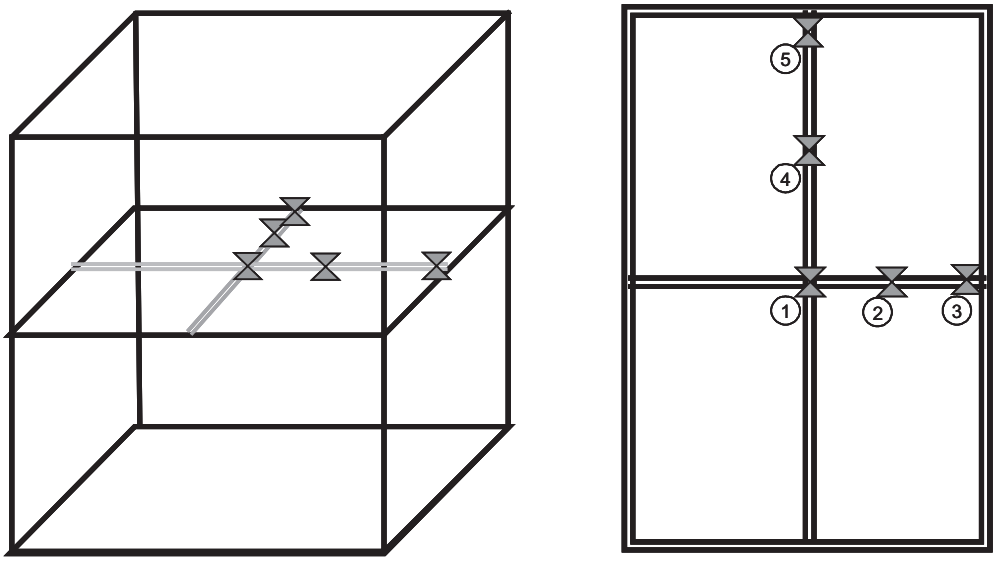


*Fig. 3. Arrangement of thermocouples in concrete section and numbering*

(*a*) initial concrete temperature, $T_i$
(*b*) maximum temperature, $T_{max}$
(*c*) the time to reach the maximum temperature
(*d*) mean ambient temperature, $T_b$
(*e*) measured $T_1$ values = $(T_{max} - T_b)$.

The effects of cement heat class, cement content, formwork type and section thickness on the temperature rise of the concrete elements are discussed in the following sections.

*Effect of cement heat class and cement content*

The effect of cement heat class on $T_1$ values for 500 mm sections is shown in Figs 6 and 7. Clearly, the VLH cements gave lower values than the LH cements. Noticeably, the difference between the two classes of

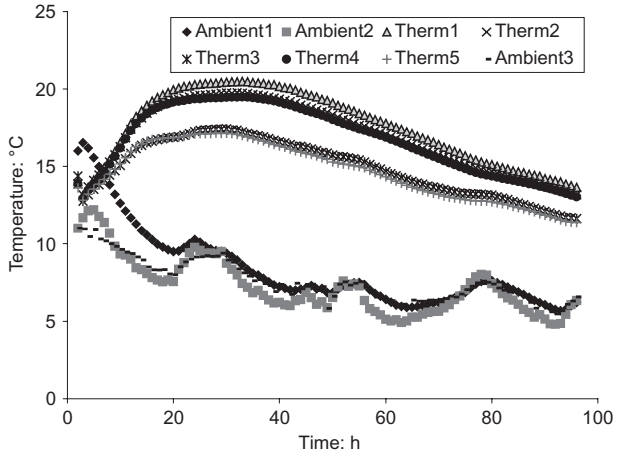


*Fig. 4. Measured temperature in concrete section at different points (A1)*

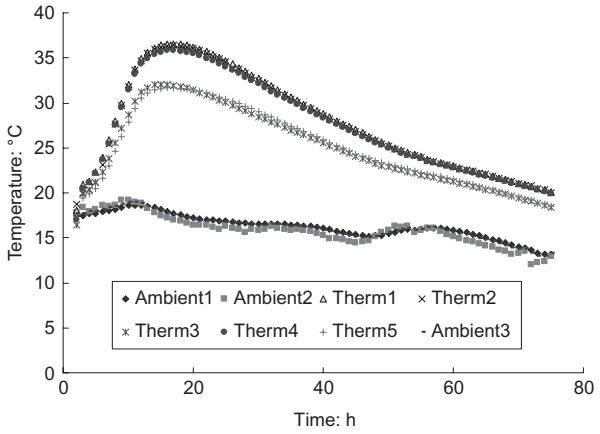


*Fig. 5. Measured temperature in concrete section at different points (E1)*

cement was more pronounced for concretes containing lower cement contents. For example, for PC/ggbs concrete at a cement content of 250 kg/m$^3$, VLH cement gave a 35–40% lower $T_1$ than the LH cements; however, for 400 kg/m$^3$, $T_1$ was only 25% lower. For PC/fly ash concretes (Fig. 7) the differences were 30% and 12%, respectively. It should be noted that element G3, constructed with 400 kg/m$^3$ VLH PC/fly ash cement in plywood formwork, gave a higher $T_1$ value than the corresponding LH PC/fly ash concrete column; this is most likely a test error.

For a given class of cement, $T_1$ values increased with an increase in cement content. In terms of percentage increase, concretes containing VLH cements were more sensitive to cement content than those containing LH cements. However, in terms of temperatures as given in Fig. 6, an increase in cement content from 250 to 400 kg/m$^3$ for an LH cement gave approximately 4–5°C (40%) increase in $T_1$, while for VLH cements the increase was 3–4°C (70%). Similar phenomena were noted for PC/fly ash cements.

Comparisons of $T_1$ values obtained by various combinations when used in 500 mm sections (steel formwork) against 28-day cube strength are shown in Fig. 8. This comparison shows that there is little significant difference in $T_1$ obtained using a 250 kg/m$^3$ LH cement and 400 kg/m$^3$ VLH cement. However, the difference in strength is much more significant. This would suggest that the optimum use of PC and ggbs or fly ash is to use a VLH cement at a high cement content rather than an LH cement at a low cement content: note that in this instance using a VLH cement at a high cement content results in a lower PC content within the blended cement (120 kg/m$^3$ compared with 135 kg/m$^3$).

### *Effect of formwork type*

The use of plywood formwork is shown to lead to higher $T_1$ values than steel formwork, see Figs 6 and 7 for PC/ggbs and PC/fly ash cements respectively. This may be explained by the low thermal conductivity of plywood compared with steel. In general, comparing the data for the 500 mm thick elements, the use of plywood formwork gave a $T_1$ value of 1–2°C (which is 10–12%) higher than that of the steel formwork. This is relatively low when compared to the data given in CIRIA Report 91[6] where differences of up to 100% are

*Table 5. Cube strength development and 28-day flexural strength*

| Concrete mix code | Cube strength development: N/mm$^2$ | | | | | Flexural strength: N/mm$^2$ |
|---|---|---|---|---|---|---|
| | 7 days | 28 days | 2 months | 3 months | 6 months | |
| ggbs concrete | | | | | | |
| A (VL, 70% ggbs) | 17·5 | 33·5 | 43·0 | 47·5 | 55·0 | 3·80 |
| B (VL, 70% ggbs) | 8·0 | 17·5 | 22·0 | 25·0 | 30·0 | 2·30 |
| C (L, 45% ggbs) | 24·0 | 40·0 | 49·0 | 53·0 | 61·0 | 4·50 |
| D (L, 45% ggbs) | 13·0 | 26·5 | 34·0 | 38·0 | 45·0 | 3·20 |
| Fly ash concrete | | | | | | |
| E (VL, 50% fly ash) | 17·5 | 28·0 | 34·0 | 37·0 | 42·0 | 3·20 |
| F (VL, 50% fly ash) | 6·0 | 12·0 | 15·5 | 17·5 | 20·5 | 1·00 |
| G (L, 30% fly ash) | 20·0 | 31·0 | 37·0 | 41·0 | 46·0 | 3·60 |
| H (L, 30% fly ash) | 8·0 | 15·0 | 18·0 | 20·0 | 23·0 | 1·40 |

*Table 6. Results of PC/ggbs concrete column tests*

| Column | $T_i$: °C | $T_{max}$: °C | $t_{,Tmax}$: h | $T_b$: °C | Measured $T_1$: °C | Predicted $T_1$: °C |
|---|---|---|---|---|---|---|
| A1 | 12·0 | 20·5 | 33 | 9·3 | 11·2 | 12·7 |
| A2 | 12·0 | 17·5 | 15 | 9·3 | 8·2 | 5·8 |
| A3 | 12·0 | 18·5 | 21 | 9·3 | 9·2 | 8·3 |
| A4 | 12·0 | 16·4 | 16 | 9·3 | 7·1 | 6·4 |
| B1 | 9·0 | 13·2 | 18 | 7·0 | 6·2 | 6·2 |
| B2 | 9·0 | 11·8 | 13 | 7·0 | 4·8 | 3·1 |
| B3 | 9·0 | 12·2 | 17 | 7·0 | 5·2 | 4·3 |
| B4 | 9·0 | 11·0 | 12 | 7·0 | 4·0 | 3·7 |
| C1 | 10·0 | 21·0 | 26 | 8·8 | 12·2 | 13·6 |
| C2 | 10·0 | 22·8 | 26 | 8·8 | 14·0 | 15·4 |
| C3 | 10·0 | 19·6 | 19 | 8·8 | 10·8 | 9·9 |
| C4 | 10·0 | 14·8 | 19 | 8·8 | 6·0 | 6·3 |
| D1 | 11·0 | 18·1 | 20 | 9·3 | 8·8 | 8·0 |
| D2 | 11·0 | 18·0 | 19 | 9·3 | 8·7 | 9·0 |
| D3 | 11·0 | 16·7 | 16 | 9·3 | 7·4 | 5·9 |
| D4 | 11·0 | 13·6 | 14 | 9·3 | 4·3 | 3·6 |

*Table 7. Results of PC/fly ash concrete column tests*

| Element | $T_i$: °C | $T_{max}$: °C | $t_{,Tmax}$: h | $T_b$: °C | Measured $T_1$: °C | Predicted $T_1$: °C |
|---|---|---|---|---|---|---|
| E1 | 18·7 | 36·6 | 17·0 | 17·9 | 18·7 | 18·6 |
| E2 | 18·7 | 32·1 | 15·7 | 17·9 | 14·2 | 12·4 |
| E3 | 18·7 | 36·4 | 23·5 | 17·9 | 18·5 | 14·7 |
| E4 | 18·7 | 27·7 | 15·5 | 17·9 | 9·8 | 11·9 |
| F1 | 15·4 | 26·9 | 22·3 | 15·3 | 11·6 | 9·8 |
| F2 | 15·4 | 23·6 | 16·5 | 15·3 | 8·3 | 6·5 |
| F3 | 15·4 | 24·5 | 19·0 | 15·3 | 9·2 | 7·7 |
| F4 | 15·4 | 20·1 | 16·0 | 15·3 | 4·8 | 6·5 |
| G1 | 16·2 | 33·7 | 19·3 | 15·7 | 18·0 | 20·9 |
| G2 | 16·2 | 36·2 | 19·3 | 15·7 | 20·5 | 23·7 |
| G3 | 16·2 | 31·9 | 17·0 | 15·7 | 16·2 | 17·5 |
| G4 | 16·2 | 25·3 | 15·3 | 15·7 | 9·6 | 11·8 |
| H1 | 16·1 | 28·9 | 19·5 | 15·6 | 13·3 | 11·6 |
| H2 | 16·1 | 29·4 | 19·8 | 15·6 | 13·8 | 13·1 |
| H3 | 16·1 | 27·3 | 16·3 | 15·6 | 11·7 | 9·7 |
| H4 | 16·1 | 23·0 | 13·5 | 15·6 | 7·4 | 6·6 |

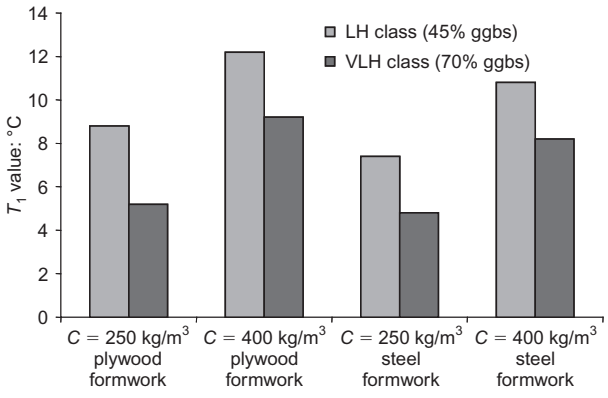


*Fig. 6. Effect of heat class on temperature rise for PC/ggbs cements (500 mm section thickness)*

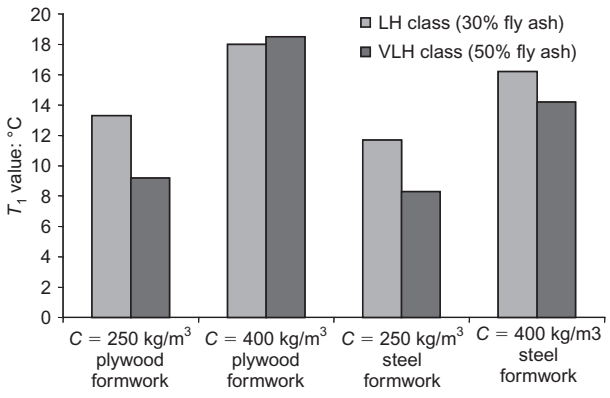


*Fig. 7. Effect of heat class on temperature rise for PC/fly ash cements (500 mm section thickness)*

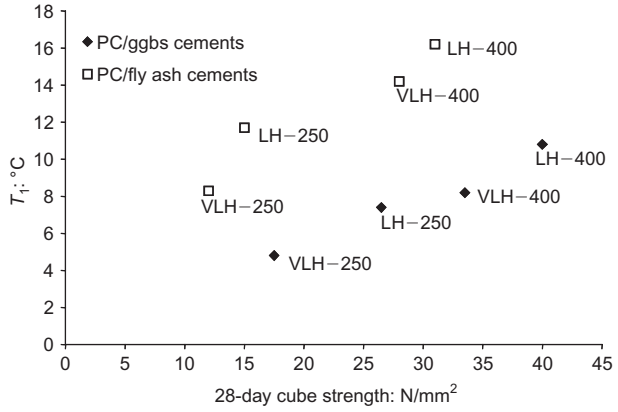


*Fig. 8. Relationship between $T_1$ value and 28-day cube strength for all cements tested (based on 500 mm section and steel formwork)*

given. This may be because the specimens were cast and stored indoors and subsequently were not exposed to the cooling effects of wind, which is known to have a greater effect on temperatures of concrete within steel formwork than that within plywood formwork.

### *Effect of section thickness*

The $T_1$ value increased with an increase in concrete section thickness in all cases. Fig. 9 compares measured data for cements meeting the LH class, and shows that the slope of the relationship between $T_1$ and section thickness reduces with section thickness.

### *Comparison with the prediction model*

Comparison of the measured $T_1$ values with those predicted by the computer program are given in Figs 10 and 11 for PC/ggbs and PC/fly ash concretes, respectively. Where the ratio of the two smallest dimensions was greater than or equal to 2, a simple one-dimensional model as described in Ref. 2 was found to be suitable and give good approximation to the measured data. For the tests described, this condition only relates to the 250 mm sections. For the 500 mm and 750 mm

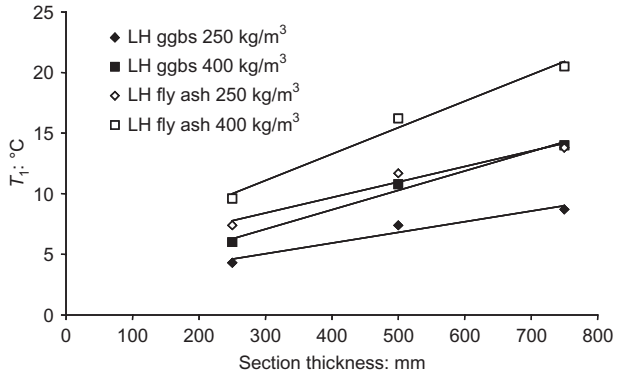


*Fig. 9. Effect of section thickness on temperature rise for LH cement combinations*

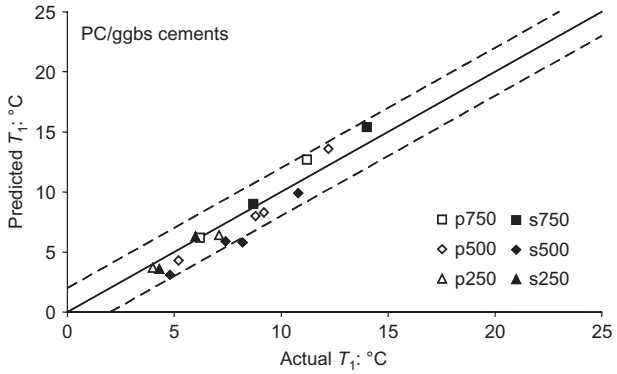


*Fig. 10. Comparison of measured data with that predicted by model for PC/ggbs cements: p—plywood formwork; s—steel formwork; the numbers are section thickness in mm*

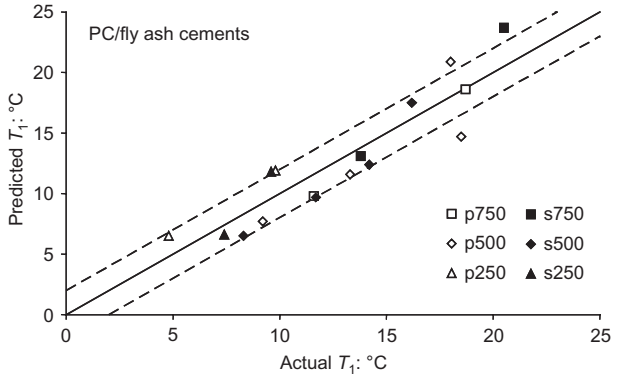


*Fig. 11. Comparison of measured data with that predicted by model for PC/fly ash cements: p—plywood formwork; s—steel formwork; the numbers are section thickness in mm*

sections, where the width-to-height ratios were 1·5 and 1·3 respectively, the one-dimensional model was found to be inaccurate. For these specimens, the two-dimensional model described in the above section 'Experimental programme of work' was used. This FEM program may also be used to predict temperature changes for other geometric elements.

These results shown in Figs 10 and 11 suggest that the model gives a good approximation for both PC/ggbs and PC/fly ash concretes with most of the elements tested falling within ±2°C of the estimated value. It is confirmed that the model and program proposed[7,8] can be used with satisfactory precision, and that the data derived for use by engineers are suitable.[29]

Further work was carried out to use the model to predict the temperature rise in real mass concrete construction in situ.

As an example, Fig. 12 shows the arrangement of three thermocouples positioned in a 1·2 m thick tunnel skin wall for a construction project in the south of England. The skin wall was cast with an LH cement comprising 50% ggbs, and was cast directly against piles and soil. Because of the irregular section, the two-dimensional FEM model was used for calculations. The

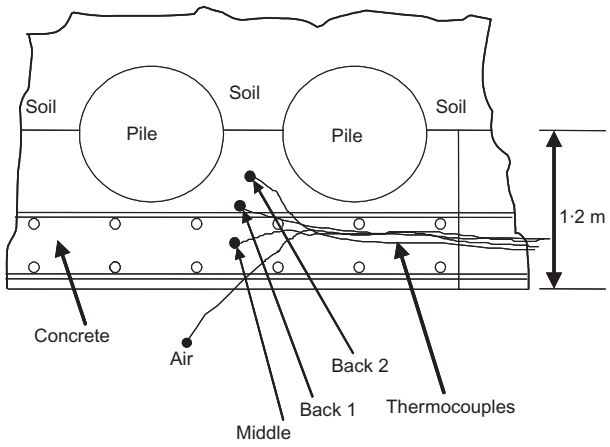


*Fig. 12. Arrangement of thermocouples in 1·2 m thick tunnel skin wall*

measured temperature data together with the predicted responses are shown in Fig. 13, and the actual and predicted maximum temperatures (and likewise the $T_1$ values) were within ±1°C. This clearly demonstrates the practical suitability of the model for real construction applications.

## Conclusions

Having measured the early-age temperature rise of 32 concrete elements, the effects of cement heat class, cement content, formwork type and section thickness on the temperature rise of the concrete elements were evaluated. VLH cements gave lower $T_1$ values than the LH cements, especially for lower cement contents. For a given class of cement, $T_1$ values increased with an increase in cement content and VLH cements appear to be more sensitive to this change. However, in terms of producing a concrete with low early-age temperature rise and high long-term strength, use of VLH cement at high cement content appears to be more effective than use of other cements at low cement content. The use of plywood formwork gave a $T_1$ value 1–2°C (10–12%) higher than that of the steel formwork in this study, which is lower than that reported in Reference 6. The $T_1$ value increased with an increase in concrete section thickness; however, in the case of large section thickness, the $T_1$ increase rate tends to diminish with a further increase in section thickness. Comparison of the measured $T_1$ values with data predicted by the model[8,9] showed that the model gives a good approximation for both PC/ggbs and PC/fly ash concretes with most of the elements tested falling within ±2°C of the estimated value.

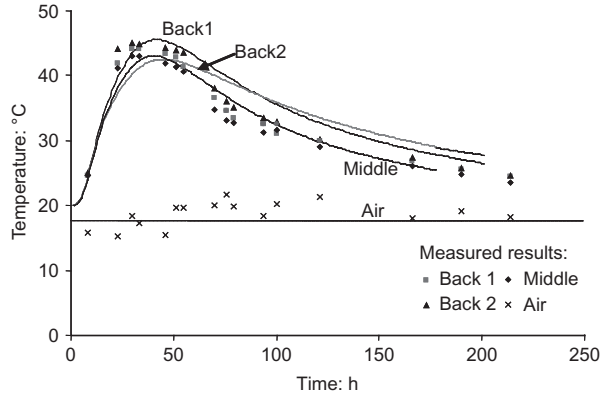


*Fig. 13. Measured (data points) and predicted (curves) temperature profile for 1·2 m thick tunnel skin wall*

## Acknowledgements

The authors would like to acknowledge the support provided by the Department of Trade and Industry, Babtie Group, British Cement Association, Castle Cement Ltd, Cementitious Slag Makers Association, Concrete Structures Group, John Doyle Construction Limited, Mott MacDonald, North of Scotland Water Authority, Quarry Products Association, Rugby Cement, ScotAsh Ltd and United Kingdom Quality Ash Association. Thanks are also given to Professor David Spooner (formerly of the British Cement Association) for supplying the prototype computer programs for concrete temperature simulation.

## References

1. British Standards Institution. *Cement. Composition, Specifications and Conformity Criteria for Common Cements*. BSI, London, 2004, BS EN 197-1.
2. British Standards Institution. *Composition, Specifications and Conformity Criteria for Low Early Strength Blast Furnace Cements*. BSI, London, 2004, BS EN 197-4.
3. British Standards Institution. *Very Low Heat Special Cements—Composition, Specifications and Conformity Criteria*. BSI, London, 2004, BS EN 14216.
4. Highways Agency. Early thermal cracking of concrete. In *Design Manual for Roads and Bridges*. Highways Agency, London, 1989, Vol. 3, section 3, BD 28/87.
5. British Standards Institution. *Code of Practice for Design of Concrete Structures for Retaining Aqueous Liquids*. BSI, London, 1987, BS 8007.
6. Harrison T. A. *Early-age Thermal Crack Control in Concrete*. Construction Industry Research and Information (CIRIA), London, 1992, Report 91.
7. Bamforth P. B. *Early-age Thermal Crack Control in Concrete*. Construction Industry Research and Information (CIRIA), London, 2007, Report C660.
8. Paine K. A., Zheng L. and Dhir R. K. Experimental study and modelling of heat evolution of blended cements. *Advances in Cement Research*, 2005, **17**, No. 5, 121–132.
9. Paine K. A., Dhir R. K. and Zheng L. Predicting early-age temperatures of blended-cement concrete. *Proceedings of the Institution of Civil Engineers, Construction Materials*, 2006, **159**, No. 4, 163–170.
10. American Society for Testing and Materials. *ASTM C595–03: 2004. Standard Specification for Blended Hydraulic*

*Cements, Annual Book of ASTM Standards V 04·01*. ASTM International, PA, USA, 2004, pp. 340–346.
11. Standards Australia. *AS 3972: 1997. Portland and Blended Cements*. Standards Australia, Homebush, NSW.
12. *GB 200: 2003. Moderate heat Portland cement, low heat Portland cement, and low heat Portland slag cement.* AQSIQ, General Administration of Quality Supervision, Inspection and Quarantine of the People's Republic of China, Beijing.
13. De Schutter G. Hydration and temperature development of concrete made with blast-furnace slag cement. *Cement and Concrete Research*, 1999, **29**, No. 1, 143–149.
14. Van Breugel K. HYMOSTRUC: a computer based simulation model for hydration and formation of structure in cement based materials. In *Hydration and Setting of Cements* (Nonat A. and Mutin J. C. (eds)). Réunion Internationale des Laboratoires et Experts des Matériaux, Systèmes de Construction et Ouvrages (RILEM). E & F N Spon, London, 1992, pp. 361–368.
15. Maekawa K., Chaube R. and Kishi T. *Modelling of Concrete Performance: Hydration, Microstructure Formation and Mass Transport*. E & F N Spon, London, 1999.
16. Bentz D. P. Three-dimensional computer simulation of Portland cement hydration and microstructure development. *Journal of the American Ceramic Society*, 1997, **80**, No. 1, 3–21.
17. Pitkänen P. Prediction of temperature fields of massive concrete structures during hardening. *Nordic Concrete Research,* 1984, **3**, 183–190.
18. Wang C. and Dilger W. H. Prediction of temperature distribution in hardening concrete. In *Thermal Cracking in Concrete at Early Ages, Proceedings of the International RILEM Symposium* (Springenschmid R. (ed.)). Institute of Building Materials, Technical University of Munich, Germany. E & F N Spon, London, 1994, pp. 21–28.
19. De Schutter G. and Taerwe L. General hydration model for Portland cement and blast-furnace slag cement. *Cement and Concrete Research*, 1995, **25**, No. 3, 593–604.
20. Carslaw H. S. and Jaeger J. C. *Conduction of Heat in Solids*, 2nd edn. Clarendon Press, Oxford, 1959, reprinted 1992.
21. Kreith F. and Bohn M. S. *Principles of Heat Transfer*, 6th edn. Brooks/Cole, Pacific Grove, California, 2001.
22. Spooner D. C. *BCA Computer Model for Temperature Rise Prediction in Fresh Concrete*. British Cement Association, TDH 51062, CIRIA, London, 1992.
23. Touzani R. *OFELI—an Object Finite Element Library.* Université Blaise Pascal, France, 2002. Reference Guide Release 1.2.2.
24. Siew P. F., Puaspansawat T. and Wu Y. H. Temperature and heat stress in a concrete column at early ages. *Australian and New Zealand Industrial and Applied Mathematics Journal*, 2003, **44**, No. E, C705–C722.
25. Dhir R. K., Paine K. A. and Zheng L. *Design Data for Low Heat and Very Low Heat Special Cements*. Concrete Technology Unit, University of Dundee, October 2006, Report CTU/4006.
26. British Standards Institution. *Specification for Ground Granulated Blastfurnace Slag for Use with Portland Cement*. BSI, London, 1992, BS 6699.
27. British Standards Institution. *Pulverized-fuel Ash: Specification for Pulverized-fuel ash for Use with Portland Cement*. BSI, London, 1997, BS 3892-1.
28. British Standards Institution. *Aggregate for Concrete.* BSI, London, 2002, BS EN 126.
29. Goodchild C. Design guidance on large area slab pours for suspended slabs. *Concrete*, 2004, **38**, No. 6, 19–22.

**Discussion contributions on this paper should reach the editor by 1 September 2008**